

Novel way of evaluating g_A quenching in β^+ /EC decays : Introducing the Branching-Ratio Method (BRM)

Aagrah Agnihotri^a, Jouni Suhonen^{a,b}

^aUniversity of Jyväskylä, P.O. Box 35 FI-40014, Jyväskylä, , Finland

^bInternational Centre for Advanced Training and Research in Physics (CIFRA), P.O. Box MG12, 077125, Bucharest-Măgurele, , Romania

Abstract

The novel Branching-Ratio Method (BRM) for the determination of effective value g_A^{eff} of the weak axial coupling g_A for forbidden non-unique (FNU) β^+ /electron-capture(EC) decays is introduced. The method offers new possibilities for testing the fitness of nuclear Hamiltonians in modeling the physics of complex β^+ /EC decays. The constraint of simultaneously reproducing the branching to β^+ and EC transitions offers an additional constraint in tackling the problem of g_A^{eff} determination. In the BRM the ambiguity in the choice of the values of g_A^{eff} and s-NME (small relativistic vector nuclear matrix element) is lifted when constraints of the branching ratios of β^+ and EC decays are applied. As an example, in the present work we apply BRM to the case of second FNU β^+ /EC decay of ^{59}Ni . This decay is treated with three different nuclear shell-model (NSM) Hamiltonians demonstrating the effects of different nuclear-structure aspects in application of the BRM.

Keywords: β^+ /electron-capture decays, Effective weak axial-vector coupling, Branching-Ratio Method, Forbidden non-unique, 2nd FNU β^+ /EC decay of ^{59}Ni

1. Introduction

Determination of the effective value of the weak axial-vector coupling g_A , i.e. g_A^{eff} , is an important problem that must be resolved in the study of weak-interaction nuclear processes [45, 44, 11, 43]. In particular, the study of neutrinoless double beta ($0\nu\beta\beta$) decay has implications concerning the foundational questions in physics [43, 7, 3, 12] and its understanding in terms of g_A^{eff} in phenomenological nuclear models is of high priority. Importance of g_A^{eff} determination for $0\nu\beta\beta$ in one of the key incentives for studying the phenomenology of g_A^{eff} for all weak-interaction nuclear processes. Further incentives for the investigation of the g_A^{eff} phenomenology include the accurate modeling of astrophysical processes [29, 30], resolving the reactor anti-neutrino flux and "bump" anomalies [20, 21, 36, 41, 48] and in determination of neutrino mass using low Q -value EC decays [4, 10, 13, 15, 35, 14, 22, 39, 40]. Practically, solving the aforementioned broad questions in physics involves understanding the two classes of weak-interaction nuclear processes, namely β^- and β^+ /electron-capture (EC) decays, as this understanding is a necessary stepping stone in resolving such questions.

The characterization of the phenomenology of g_A^{eff} has been a long-standing mystery, and only in recent years this mystery has been resolved for a restricted set of light nuclei by P. Gysbers *et al.* [16]. This work makes it clear that the need to use a renormalized value of g_A (or actually a renormalized spin-isospin operator) is the manifestation of, e.g., missing nuclear many-body correlations in the computed β -decay nuclear matrix ele-

ments (NMEs); a consequence part and parcel of using approximations, i.e. adopting nuclear models with phenomenological many-body Hamiltonians, instead of the complete *ab initio* one. The virtual impossibility of solving the nuclear many-body problem exactly in all nuclear mass regions makes the use of limited phenomenological nuclear models inevitable. Determination of g_A^{eff} is an effective and practical way to renormalize the involved spin-isospin operator across the nuclide chart for the phenomenological nuclear models [45].

Studies have been done for understanding g_A^{eff} phenomenology in allowed and first-forbidden unique β decays [45, 11, 44, 46, 19], but considerable attention has lately been paid to evaluations of g_A^{eff} in forbidden non-unique (FNU) β^- decays, in particular in terms of β -electron spectral shapes [17, 18, 23, 27, 28, 34, 38, 8, 24, 31, 32, 25, 26, 5, 37, 33]. The degree to which different flavors of β^- decays are treated in the literature, and understanding of g_A^{eff} therein, depend on the complexity and difficulty of modeling a given decay type. Some work has been lately done to understand the FNU EC decays in terms of g_A^{eff} in [2], but no general and consistent treatment for combined FNU β^+ and EC decays exists in the present literature since they are the most complex of all β decays, and therefore aspects of g_A^{eff} on this front are a terra incognita.

This letter is an attempt to pave the way for the exploration of the less discussed physics of FNU β^+ /EC decays. For this, we introduce here the novel Branching-Ratio Method (BRM) for g_A^{eff} determination that is applicable to all β^+ /EC decays. For demonstration of the power of BRM, we apply it to the 2nd FNU β^+ /EC ground-state-to-ground-state transition $^{59}\text{Ni}(3/2^-) \rightarrow ^{59}\text{Co}(7/2^-)$. The BRM for g_A^{eff} determination

Email addresses: aagrah.a.agnihotri@jyu.fi (Aagrah Agnihotri), jouni.t.suhonen@jyu.fi (Jouni Suhonen)

is different from mainstream β^- methods, like the spectrum-shape method (SSM) [17, 18], its enhanced version [27, 28] and the spectral moment method (SMM) [25, 26], in that it can be consistently applied to all β^+ /EC decays. BRM uses the relative branching ratios between the β^+ and EC sub-branches of a β^+ /EC transition to determine g_A^{eff} . This method is particularly helpful for FNU decays, but in principle equally applicable to allowed and forbidden unique (FU) decays. The essence of g_A^{eff} determination for the FNU β decays involves treating the value of g_A^{eff} as a free parameter and fitting its value to reproduce the branching ratios/(partial) half-lives and spectral shapes simultaneously. Such fitting suffices for modeling all features of allowed and FU β^- decays as well, but without the spectral-shape aspect since these decays have universal spectral shapes, independent of g_A^{eff} . In BRM the difficulty of reproducing the β^+ and EC branching ratios simultaneously is overcome with the aid of an additional free parameter, namely the small relativistic vector NME (sNME), used already in the enhanced SSM [27, 28] and SMM [25, 26]. An interesting new aspect of the sNME is that a β^- spectral shape may also depend strongly on the sNME itself [27, 28, 34, 38]. Hence, two experimental constraints are always needed for FNU decays to determine g_A^{eff} and sNME simultaneously.

BRM is a powerful tool to test the suitability of nuclear Hamiltonians for description of weak-interaction processes, in particular the β decays. Here g_A^{eff} and sNME can be determined by the total branching of a β^+ /EC transition and the relative branching of β^+ and EC in this transition. A severe check of the consistency of this fitting is the comparison of the resulting positron spectral shape with the measured one. This is the more rewarding if the spectral shape would depend on g_A^{eff} and/or sNME. Such a double check would qualify a phenomenological or an *ab initio* Hamiltonian with considerable confidence. Such exposure of the imperfections of the adopted Hamiltonians will help improve the quality of nuclear-structure models.

2. Theory

2.1. Theory of β decay

The non-relativistic limit of the theory of β decays is well established and a detailed account is presented in [6]. A more concise and practical exposition of the treatment of forbidden β^+ /EC decays is given in [47]. The half-life value for β^+ /EC decays, $t_{1/2}^{\beta^+/\text{EC}}$, is given as

$$t_{1/2}^{\beta^+/\text{EC}} = \frac{\kappa}{\tilde{C}^{\beta^+} + \tilde{C}^{\text{EC}}}, \quad (1)$$

where κ takes the value of 6289 s. \tilde{C}^{β^+} and \tilde{C}^{EC} are the integrated shape functions of β^+ and EC decays, respectively. The integrated shape function of forbidden non-unique β^-/β^+ decay is given as

$$\tilde{C}^\mp = \int_1^{w_0} C^\mp(w_e) p w_e (w_0 - w_e)^2 F_0(\pm Z_f, w_e) dw_e, \quad (2)$$

where w_e is the total energy of the emitted electron/positron and p is the electron/positron momentum, scaled by the electron rest mass. Here Z_f is the charge number of the daughter

nucleus, and $F_0(Z_f, w_e)$ is the Fermi function. The integrated shape function for EC decay can be written as [47]

$$\tilde{C}^{\text{EC}} = \frac{\pi}{2} \sum_{x=1s,2s} n_x \beta_x^2 (p_{v_x}/m_e c)^2 C(p_{v_x}), \quad (3)$$

when considering the leading channels, namely K capture (1s) and L_1 capture (2s). Here n_x are relative occupancies for the respective orbitals, β_x are the electron Coulomb amplitudes, and p_{v_x} is the momentum of the neutrino when the electron is captured from the atomic orbital x [47]. The shape factor $C(p_{v_x})$ used in Eq. (3), containing complicated combinations of phase-space factors and nuclear matrix elements (NMEs), is given for forbidden EC transitions in detail in [47].

According to Eq. 1, the (partial) half-life $t_{1/2}^{\beta^+/\text{EC}}$ of the β^+ /EC decay transition is related to the partial half-lives $t_{1/2}^{\beta^+}$ and $t_{1/2}^{\text{EC}}$ of its β^+ and EC sub-branches, respectively, as:

$$\frac{1}{t_{1/2}^{\beta^+/\text{EC}}} = \frac{1}{t_{1/2}^{\beta^+}} + \frac{1}{t_{1/2}^{\text{EC}}}. \quad (4)$$

In case of a β^+ /EC transition between two nuclear states, the total branching ratio is given as:

$$\text{BR}_{\beta^+/\text{EC}}\% = \frac{T_{1/2}^{\text{tot}}}{t_{1/2}^{\beta^+/\text{EC}}} \times 100, \quad (5)$$

with $T_{1/2}^{\text{tot}}$ being the total β^+ /EC half-life of the parent nucleus. The branching ratios of β^+ and EC sub-branches of a given β^+ /EC transition, with total half-life $t_{1/2}^{\beta^+/\text{EC}}$, are given in a similar way as outlined in Eq. (5), thus being

$$\text{BR}_{\beta^+}\% = \frac{t_{1/2}^{\beta^+/\text{EC}}}{t_{1/2}^{\beta^+}} \times 100, \quad \text{BR}_{\text{EC}}\% = \frac{t_{1/2}^{\beta^+/\text{EC}}}{t_{1/2}^{\text{EC}}} \times 100. \quad (6)$$

Finally, following Eq. (6), we define the relative branching ratio of the β^+ sub-branch with respect to the EC sub-branch for a given β^+ /EC transition as

$$\text{BR}_{\beta^+:\text{EC}} = \frac{\text{BR}_{\beta^+}}{\text{BR}_{\text{EC}}} = \frac{t_{1/2}^{\text{EC}}}{t_{1/2}^{\beta^+}}. \quad (7)$$

Computed average β energy, $\langle E_{\beta^\mp} \rangle$, for β^\mp decays, can also be relevant when speculating the physical relevance of a β spectral-shape prediction. One can compute $\langle E_{\beta^\mp} \rangle$ using the integrated shape function of Eq. (2) using the following relation:

$$\langle E_{\beta^\mp} \rangle = \frac{\int_0^{E_0} E \times \tilde{C}^\mp dE}{\int_0^{E_0} \tilde{C}^\mp dE} \quad (8)$$

where E is the kinetic energy of the β particle and E_0 is the β end-point energy.

2.2. Branching-Ratio Method (BRM) for β^+ /EC decays

As alluded to in the introduction, the Branching-Ratio Method (BRM) for g_A^{eff} determination in a β^+ /EC decay transition involves necessarily applying a measured relative branching ratio, defined by Eq. (7), as a constraint to theoretical computations and the fit of g_A^{eff} as a free parameter. The basis of the

BRM is the physical assumption that theoretical NMEs must reproduce simultaneously the partial half-life $t_{1/2}^{\beta^+/\text{EC}}$ of the β^+/EC decay transition of interest (in case of just one possible transition this is the total half-life $T_{1/2}^{\text{tot}}$ of the mother nucleus) and the relative branching of Eq. (7). The β^+/EC decays are sensitive to imperfections/incompleteness of NME of phenomenological nuclear models and depend non-trivially on g_A^{eff} (and sNME in case of FNU decays). Therefore, $\text{BR}_{\beta^+:\text{EC}}$ of Eq. (7) is a demanding experimental observable to reproduce theoretically; yet for exactly the same reason, it makes for an excellent test and standard for improving the quality of phenomenological nuclear models and Hamiltonians.

It should be noted here that for a FNU β^+/EC transition the simultaneous BRM description of both the half-life of the β^+/EC transition of interest and the relative branching of Eq. (7) is highly non-trivial and can succeed or fail for a phenomenological Hamiltonian. For the FNU decays the sNME can be brought in as an additional parameter, as done in the enhanced SSM [27, 28] and SMM [25, 26]. However, even this does not guarantee a successful application of the BRM, as shown below by our example Hamiltonians in the case of the FNU β^+/EC decay of ^{59}Ni . A rough guess for the value of sNME is its CVC-based value, sNME_{CVC} , obtained by relating the value of sNME to the value of a large vector NME, INME, as described, e.g., in Refs. [25, 26]. This value of sNME pertains, however, to an ideal many-body nuclear theory and thus serves only as a rough reference for the sNME values obtained in the BRM for the imperfect phenomenological nuclear Hamiltonians.

Potential cross check of the BRM is the measurement of the β^+ -decay positron spectrum. The related positron spectral shape gives an extra constraint for the BRM-extracted values of g_A^{eff} and sNME, be it dependent or independent of g_A^{eff} . For a perfect model Hamiltonian all three constraints, namely the β^+/EC half-life and relative branching as also the positron spectral shape should be simultaneously reproduced by a unique pair of values (g_A^{eff} , sNME). For an imperfect Hamiltonian the three experimental observables open up several ways to explore the physical content of the Hamiltonian and thus gain understanding for future improvements of it. Hence, measurements of the positron spectral shapes are welcome for validation and improvement of Hamiltonians of both phenomenological and *ab initio* nuclear models.

3. Calculations and results

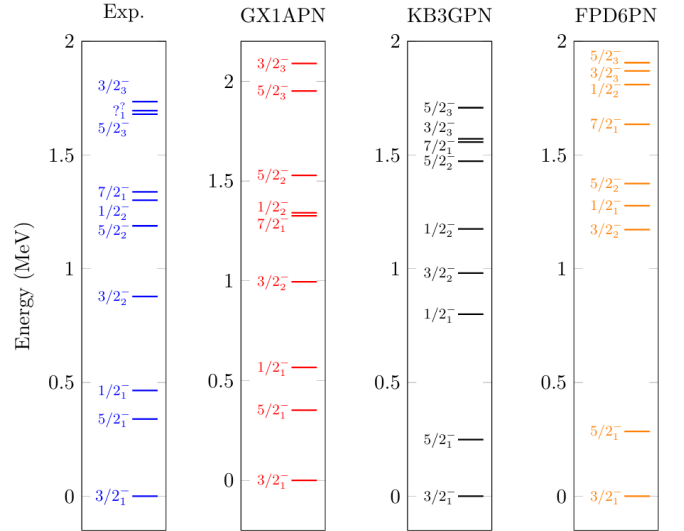
3.1. Nuclear-Structure Calculations

Nuclear wave functions for the NMEs and electromagnetic (EM) observables are computed using the NSM computer program NuShellX@MSU [9]. For the parent and daughter nuclei three well-established nuclear Hamiltonians in the PFPN model space are used to draw out different nuclear-structure manifestations of the same β^+/EC decay transition through the lens of the BRM. The three Hamiltonians correspond to three interactions namely GX1APN, KB3GPN, and FPD6PN. The computed energy-level schemes for ^{59}Ni (parent nucleus) and ^{59}Co (daughter nucleus) are given in Fig.1 and Fig.2, respectively. In

Table 1: Experimental and theoretical values of EM moments of the states involved in the β^+/EC decay of ^{59}Ni . The magnetic dipole (μ) and electric quadrupole (Q) moments are given in units of nuclear magnetons (μ_N/c) and ebarns, respectively. In the calculations, an effective charge $1.5e$ ($0.5e$) for proton (neutron) and bare g factors were used [42]. Experimental values are taken from [1].

Interaction	μ_{exp}	μ_{theo}	Q_{exp}	Q_{theo}
$^{59}\text{Ni}_{31}(3/2^-)$				
GX1APN	-	-0.632	-	+0.0662
KB3GPN	-	-1.083	-	-0.0163
FPD6PN	-	-0.657	-	-0.1486
$^{59}\text{Co}_{32}(7/2^-)$				
GX1APN	+4.615(25)	+4.543	+0.42(3)	+0.4407
KB3GPN		+4.398		+0.3946
FPD6PN		+4.544		+0.4678

Figure 1: Comparison of the experimental and GX1APN-, KB3GPN- and FPD6PN-computed level energies (in MeV) of ^{59}Ni .

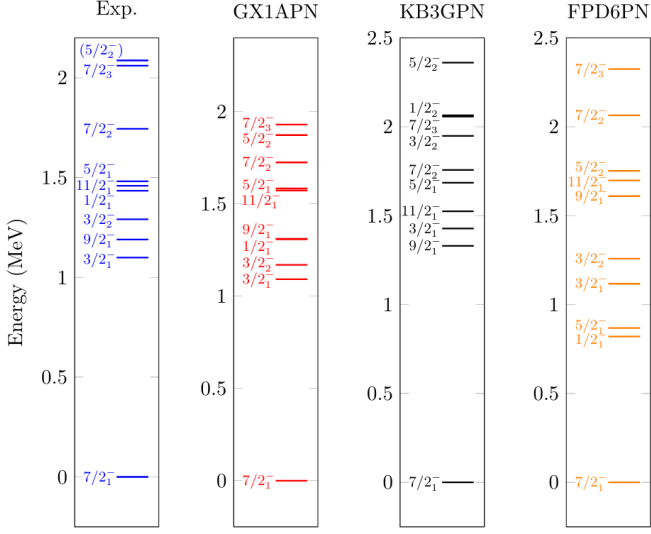


general, the experimental level energies are reproduced rather well for all interactions, with the GX1APN interaction giving the best and quite nice agreement between theory and experiment. In table 1, magnetic dipole and electric quadrupole moments of the ground states of ^{59}Ni and ^{59}Co are given for the three interactions. Experimental values of EM moments of the ground states are known only for ^{59}Co , and again the GX1APN interaction gives the best estimates for the observables.

3.2. BRM for the Hamiltonians GX1APN, KB3GPN and FPD6PN

As discussed in section 2.2, one can fit the free parameters to the experimental partial half-lives $t_{1/2}^{\beta^+/\text{EC}}$, $t_{1/2}^{\beta^+}$ and $t_{1/2}^{\text{EC}}$ through the β^+/EC -decay half-life $t_{1/2}^{\beta^+/\text{EC}}$ and the relative branching of Eq. (7). For the FNU β^+/EC decay ground-state-to-ground-state transition $^{59}\text{Ni}(3/2^-) \rightarrow ^{59}\text{Co}(7/2^-)$ the fitting of $t_{1/2}^{\beta^+/\text{EC}}$

Figure 2: Comparison of the experimental and GX1APN-, KB3GPN- and FPD6PN-computed level energies (in MeV) of ^{59}Co .

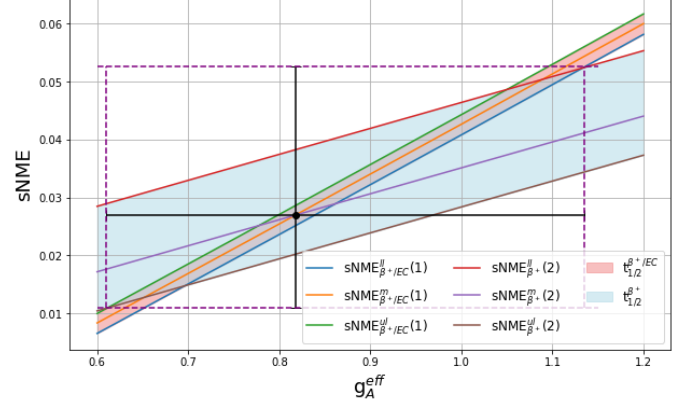


will result in a pair of sNME values for each g_A^{eff} , labeled $\text{sNME}_{\beta^+/\text{EC}}(1)$ and $\text{sNME}_{\beta^+/\text{EC}}(2)$ due to the existence of two sNME solutions for a given g_A^{eff} [32, 24, 25, 26, 8, 34, 38, 5, 37]. The Q-value of the decay under study is 1073.00(19) keV [1], with strong EC feeding and very weak β^+ feeding. The BR_{β^+} and BR_{EC} are $3.7(12)\times 10^{-7}$ and 0.9999696(1) [1], respectively, corresponding to $t_{1/2}^{\beta^+} = 6.48_{-2.15}^{+2.15}\times 10^{18}$ s and $t_{1/2}^{\text{EC}} = 2.40_{-0.16}^{+0.16}\times 10^{12}$ s. Clearly, the relative branching ratio (7) will practically be the same as BR_{β^+} , hence we take its value to be $3.7(12)\times 10^{-7}$. Also, $t_{1/2}^{\text{EC}}$ and $t_{1/2}^{\beta^+/\text{EC}}$ are practically the same for the purposes of model calculations, therefore we take both values to be the same.

Given the above premises, we proceed to discuss the strategy to address the half-lives $t_{1/2}^{\beta^+/\text{EC}}$ and $t_{1/2}^{\beta^+}$ and the relative branching $\text{BR}_{\beta^+/\text{EC}}$ of Eq. (7), including their experimental error bands by using the GX1APN interaction. For this we define two independent sNME: $\text{sNME}_{\beta^+/\text{EC}}$ and sNME_{β^+} . We fit g_A^{eff} and $\text{sNME}_{\beta^+/\text{EC}}$ to reproduce the experimental half-life $t_{1/2}^{\beta^+/\text{EC}}$ with its error band. The resulting fitted values, $\text{sNME}_{\beta^+/\text{EC}}(1)$ and $\text{sNME}_{\beta^+/\text{EC}}(2)$, together with the resulting relative branchings, are displayed in table 2 in rows 2 - 6. We can also fit g_A^{eff} and sNME_{β^+} to reproduce the experimental half-life $t_{1/2}^{\beta^+}$ with its error band. The corresponding fitted values, $\text{sNME}_{\beta^+}(1)$ and $\text{sNME}_{\beta^+}(2)$, together with the resulting relative branchings, are displayed in table 2 in rows 8 - 12.

First important thing that is observed from these results, is that the two sNME solutions, $\text{sNME}_X(1)$ and $\text{sNME}_X(2)$, $X = \beta^+/\text{EC}, \beta^+$, always produce different orders of magnitude for the relative branching. This fact speaks for the utility of the relative BR in determining the physically relevant sNME value when compared with the experimental value. It is seen from these results that branching ratios of β^+ and EC sub-branches need not be simultaneously reproduced using the computed

Figure 3: Experimental mean values and error bands for the half-lives $t_{1/2}^{\beta^+/\text{EC}}$ (red) and $t_{1/2}^{\beta^+}$ (blue), and the resulting lower limits (ll), mean values (m) and upper limits (ul) for $\text{sNME}_{\beta^+/\text{EC}}$ and sNME_{β^+} . The overlap region defines the physically relevant values of sNME and g_A^{eff} , as indicated by the horizontal and vertical bars centered at the mean values of the involved sNME(1) and sNME(2).



$\text{sNME}_{\beta^+/\text{EC}}$. Existence or non-existence of $\text{sNME}_{\beta^+/\text{EC}}$ for a given g_A^{eff} that simultaneously reproduces the relative branching is dependent on the adopted nuclear model. We see from the results in rows 2 - 6 that for the GX1APN interaction, the experimental relative BR is reached only for the $\text{sNME}_{\beta^+/\text{EC}}(1)$ subset for $g_A^{\text{eff}} = 0.818$ and $\text{sNME}_{\beta^+/\text{EC}}(1) = 0.02697_{-0.00182}^{+0.00163}$. Similarly, from the results in rows 8 - 12 we see that the experimental relative BR is reached only for the $\text{sNME}_{\beta^+}(2)$ subset for $g_A^{\text{eff}} = 0.818$ and $\text{sNME}_{\beta^+}(2) = 0.02697_{-0.00647}^{+0.01123}$. The significant experimental uncertainty in the half-lives $t_{1/2}^{\beta^+/\text{EC}}$ and $t_{1/2}^{\beta^+}$, leads to a significant uncertainty in the values of g_A^{eff} and sNME determined using the BRM. The upper/lower bounds of the possible g_A^{eff} and sNME values can be determined upon applying the constraints of upper/lower bounds of $t_{1/2}^{\beta^+}$ and $t_{1/2}^{\beta^+/\text{EC}}$ as shown in figure 3. This yields $g_A^{\text{eff}} \in [0.61, 1.135]$ and $\text{sNME} \in [0.011, 0.0525]$ for the physically acceptable ranges of these parameters. Within these ranges the measured values of $t_{1/2}^{\beta^+/\text{EC}}$ and $t_{1/2}^{\beta^+}$ are simultaneously reproduced, the central values being $g_A^{\text{eff}} = 0.818$ and $\text{sNME} = 0.0270$, and the associated ranges being $g_A^{\text{eff}} = 0.818_{-0.208}^{+0.317}$ and $\text{sNME} = 0.0270_{-0.016}^{+0.0255}$. The latter values deviate notably from the CVC-determined value $\text{sNME}_{\text{CVC}} = 0.175$.

Table 2: GX1APN-computed sNME values, $s\text{NME}_{\beta^+/\text{EC}(1)}$ and $s\text{NME}_{\beta^+/\text{EC}(2)}$, columns 2 and 4, which reproduce the experimental total half-life (rows 2 - 6) or the β^+ half-life (rows 8 - 12) for a given g_A^{eff} of the 2nd FNU β^+/EC decay transition of ^{59}Ni . The respective relative BR, $\text{BR}_{\beta^+:\text{EC}}$, are also given in columns 3 and 5. The last row gives the CVC value of sNME.

g_A^{eff}	$s\text{NME}_{\beta^+/\text{EC}(1)}$	$\text{BR}_{\beta^+:\text{EC}}$	$s\text{NME}_{\beta^+/\text{EC}(2)}$	$\text{BR}_{\beta^+:\text{EC}}$
0.6	$0.00839^{+0.00163}_{-0.0018}$	$2.52^{+0.38}_{-0.37}\text{e-}7$	$0.10703^{+0.00163}_{-0.00179}$	$2.87^{+0.12}_{-0.12}\text{e-}6$
0.8	$0.02543^{+0.00164}_{-0.00181}$	$3.60^{+0.50}_{-0.48}\text{e-}7$	$0.12344^{+0.00164}_{-0.00181}$	$3.19^{+0.14}_{-0.14}\text{e-}6$
0.818	$0.02697^{+0.00163}_{-0.00182}$	$3.71^{+0.50}_{-0.50}\text{e-}7$	$0.12491^{+0.00164}_{-0.00181}$	$3.21^{+0.14}_{-0.14}\text{e-}6$
1.0	$0.04260^{+0.00163}_{-0.00183}$	$4.89^{+0.63}_{-0.61}\text{e-}7$	$0.13972^{+0.00167}_{-0.00183}$	$3.51^{+0.16}_{-0.16}\text{e-}6$
1.2	$0.05992^{+0.00167}_{-0.00185}$	$6.41^{+0.78}_{-0.76}\text{e-}7$	$0.15585^{+0.00167}_{-0.00185}$	$3.85^{+0.17}_{-0.17}\text{e-}6$
	$s\text{NME}_{\beta^+}(1)$		$s\text{NME}_{\beta^+}(2)$	
0.6	$-0.08301^{+0.00673}_{-0.0127}$	$4.70^{+0.81}_{-0.73}\text{e-}8$	$0.01720^{+0.00673}_{-0.0127}$	$5.39^{+2.37}_{-1.93}\text{e-}7$
0.8	$-0.07414^{+0.00673}_{-0.01126}$	$4.21^{+0.74}_{-0.73}\text{e-}8$	$0.02616^{+0.00673}_{-0.01126}$	$3.81^{+1.38}_{-1.56}\text{e-}7$
0.818	$-0.07334^{+0.00673}_{-0.01125}$	$4.17^{+0.73}_{-0.73}\text{e-}8$	$0.02697^{+0.00673}_{-0.01123}$	$3.71^{+1.34}_{-1.54}\text{e-}7$
1.0	$-0.06524^{+0.00673}_{-0.01126}$	$3.80^{+0.69}_{-0.69}\text{e-}8$	$0.03509^{+0.00673}_{-0.01126}$	$2.82^{+1.12}_{-1.12}\text{e-}7$
1.2	$-0.05632^{+0.00673}_{-0.01126}$	$3.44^{+0.63}_{-1.07}\text{e-}8$	$0.04400^{+0.00673}_{-0.01126}$	$2.17^{+0.82}_{-1.07}\text{e-}7$
	$s\text{NME}_{\text{CVC}}=0.175$			

At this point it should be noted that the other two test Hamiltonians, KB3GPN and FPD6PN, could not perform successfully when applying the BRM: Neither one could reproduce simultaneously the experimental partial half-lives $t_{1/2}^{\beta^+/\text{EC}}$ and $t_{1/2}^{\beta^+}$, i.e. no unique pair (g_A^{eff} , sNME) could be found to explain the central values of both half-lives. Hence, it can be said that GX1APN is the best interaction of the available three for the description of β^+/EC decay properties in this case. This is in line with the finding that also the electromagnetic moments were found to be best reproduced by this interaction in section 3.1.

3.3. β spectra

Out of twelve subsets of sNME values (four for each adopted Hamiltonian), only one subset, corresponding to $s\text{NME}_{\beta^+/\text{EC}(2)}$ for the KB3GPN interaction, shows g_A^{eff} /sNME dependence of the positron spectral shape, presented in Fig. 4a. The spectra for the remaining eleven subsets are g_A^{eff} /sNME independent and practically have the same spectral shape, and we refer to this shape as the universal "default" shape. Therefore, a showcase spectral shape for the GX1APN and FPD6PN interactions is given for reference in Fig. 4b, corresponding to $g_A^{\text{eff}}=1.0$. In Table 3, the ranges of average positron energies $\langle E_{\beta^+} \rangle$ of Eq. (8), corresponding to the spectral shapes of Fig. 4, are presented. Here each spectral shape corresponds to a unique $\langle E_{\beta^+} \rangle$. The visible trend, as seen in Fig. 4a and Table 3, is that as g_A becomes less quenched, the spectral shape approaches the "default" shape presented in Fig. 4b. Therefore the primary prediction for the spectral shape would be the "default" shaped spectrum, valid for $g_A^{\text{eff}} = 0.818^{+0.317}_{-0.208}$ and $s\text{NME} = 0.0270^{+0.0255}_{-0.016}$ as determined in Sec. 3.2 using the GX1APN interaction.

4. Summary and conclusions

To summarize, in this letter a novel and powerful method, namely the Branching Ratio Method (BRM), is introduced for g_A^{eff} determination for β^+/EC decays. As an example, the BRM is applied in modeling the physics of 2nd FNU β^+/EC decay of

Figure 4: Computed spectral-shape predictions for the three interactions under consideration. The labels lower limits (ll), mean values (m) and upper limits (ul) are for sNME values for a given g_A^{eff} obtained upon fitting to uncertainty limits of the total half-life $t_{1/2}^{\beta^+/\text{EC}}$. The spectral shape depicted in panel (b) is "universal" corresponding to all values of g_A^{eff} , $s\text{NME}_{\beta^+/\text{EC}(1)}$ and $s\text{NME}_{\beta^+/\text{EC}(2)}$ for the interactions GX1APN and FPD6PN, with $g_A^{\text{eff}} = 1$ and $s\text{NME}_{\beta^+/\text{EC}(2)}$ taken as a showcase.

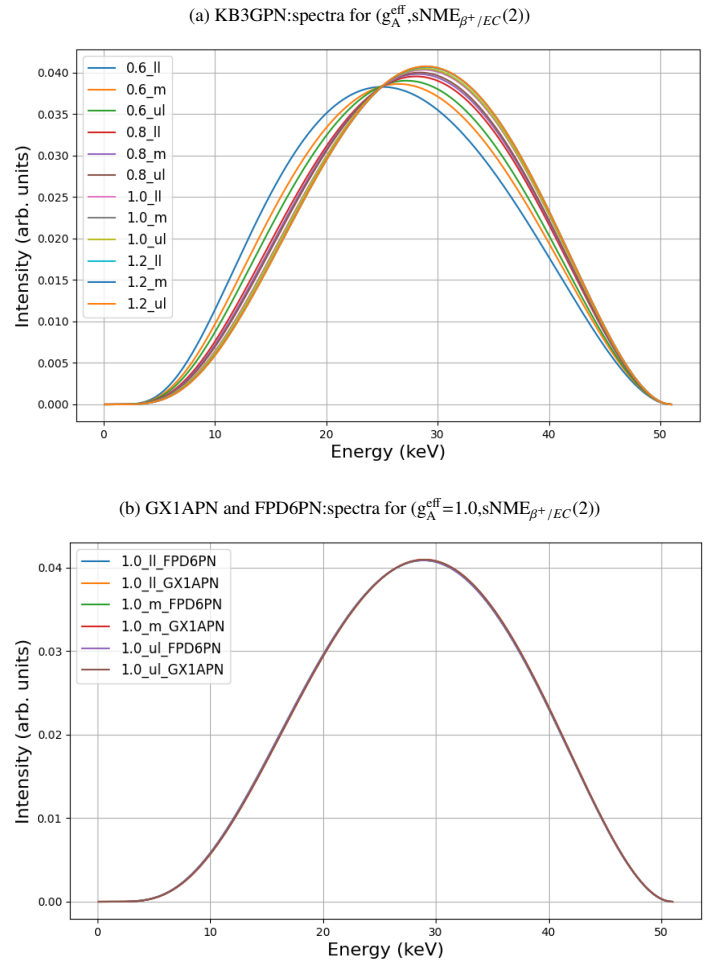


Table 3: The average positron energies $\langle E_{\beta^+} \rangle$ corresponding to computed spectral shapes presented in Fig. 4

KB3GPN		
g_A^{eff}	sNME $_{\beta^+/\text{EC}}(2)$	$\langle E_{\beta^+} \rangle$
0.6	$0.01943_{-0.00161}^{+0.00179}$	$26.92_{-0.68}^{+0.38}$
0.8	$0.01073_{-0.0018}^{+0.00162}$	$27.93_{-0.15}^{+0.09}$
1.0	$0.001938_{-0.00181}^{+0.00163}$	$28.28_{-0.02}^{+0.04}$
1.2	$-0.00698_{+0.00165}^{-0.00184}$	$28.43_{-0}^{+0.01}$
GX1APN		
g_A^{eff}	sNME $_{\beta^+/\text{EC}}(2)$	$\langle E_{\beta^+} \rangle$
1.0	$0.13972_{+0.00183}^{-0.00165}$	28.47_{+0}^{-0}
FPD6PN		
g_A^{eff}	sNME $_{\beta^+/\text{EC}}(2)$	$\langle E_{\beta^+} \rangle$
1.0	$0.05715_{+0.00181}^{-0.00164}$	$28.64_{+0.01}^{-0}$

^{59}Ni . Using the BRM it becomes clear that out of the three Hamiltonians, GX1APN is the best interaction as it is the one that reproduces the experimental value of the branching ratio $\text{BR}_{\beta^+/\text{EC}}$ of Eq. (7) and the experimental total half-life $t_{1/2}^{\beta^+/\text{EC}}$ simultaneously. A powerful aspect of the BRM becomes evident in the case of 2^{nd} FNU β^+/EC decay of ^{59}Ni from its ability to differentiate between two sNME solutions that reproduce the (partial) half-lives of Eq. (4), since the values of $\text{BR}_{\beta^+/\text{EC}}$ for the two sNME values are of different orders of magnitude for all the adopted interactions. Such differentiation helps identify the physically relevant sNME making it possible to determine g_A^{eff} uniquely, as in the case of the GX1APN interaction. In the present case, the values $g_A^{\text{eff}} = 0.818_{-0.208}^{+0.317}$ and $\text{sNME} = 0.0270_{-0.016}^{+0.0255}$ are determined with significant uncertainty consequent of the large uncertainties in the (partial) half-lives of Eq. (4) to which the two parameters are fitted.

It would be interesting and important to compare our obtained "default" positron spectral shape with a measured one in order to have a further confirmation of the suitability of the GX1APN interaction for reliable prediction of beta-decay properties of the p - f -shell nuclei. Furthermore, we could show that the other two interactions, KB3GPN and FPD6PN, studied in this work, have clear shortcomings in this respect. The here studied KB3GPN interaction is a showcase of g_A -dependent positron spectral shapes and as such amenable to the enhanced SSM (spectrum-shape method) or SMM (spectral-moments method) type of determination of g_A^{eff} , never conducted in the β^+/EC side of nuclear β decays. The complementary aspects and interplay between the BRM, enhanced SSM, and SMM remain an interesting open question as experiments are necessary for such studies to determine the spectral shape for FNU β^+/EC

decays. The branching-ratio method could usher a renaissance in our understanding of the β^+/EC decays, while simultaneously testing the suitability and limitations of nuclear Hamiltonians in modeling weak-interaction processes relevant for the neutrinoless double beta decay, nuclear astrophysics, reactor neutrinos and small-decay-energy beta decays.

Acknowledgements

We acknowledge support from project PNRR-I8/C9-CF264, Contract No. 760100/23.5.2023 of the Romanian Ministry of Research, Innovation and Digitization (the NEPTUN project). We acknowledge grants of computer capacity from the Finnish Grid and Cloud Infrastructure (persistent identifier urn:nbn:fi:research-infras-2016072533).

References

- [1] ENSDF database. *National Nuclear Data Center (NNDC)*, 2024. URL <https://www.nndc.bnl.gov/ensdf/>.
- [2] Aagrah Agnihotri, Jouni Suhonen, and Hong Joo Kim. Constraints for rare electron-capture decays mimicking detection of dark-matter particles in nuclear transitions. *Phys. Rev. Lett.*, 133:232501, Dec 2024. doi: 10.1103/PhysRevLett.133.232501.
- [3] Matteo Agostini, Giovanni Benato, Jason A. Detwiler, Javier Menéndez, and Francesco Vissani. Toward the discovery of matter creation with neutrinoless $\beta\beta$ decay. *Rev. Mod. Phys.*, 95:025002, 2023.
- [4] M. Aker, *et al.*, and (The KATRIN Collaboration). Direct neutrino-mass measurement with sub-electronvolt sensitivity. *Nat. Phys.*, 18:160–166, 2022. doi: <https://doi.org/10.1038/s41567-021-01463-1>.
- [5] I. Bandac, L. Bergé, J. M. Calvo-Mozota, P. Carniti, M. Chapellier, F. A. Danevich, T. Dixon, L. Dumoulin, F. Ferri, A. Giuliani, C. Gotti, Ph. Gras, D. L. Helis, L. Imbert, H. Khalife, V. V. Kobychyev, J. Kostensalo, P. Loaiza, P. de Marcillac, S. Marnieros, C. A. Marrache-Kikuchi, M. Martinez, C. Nones, E. Olivieri, A. Ortiz de Solórzano, G. Pessina, D. V. Poda, J. A. Scarpaci, J. Suhonen, V. I. Tretyak, M. Zarytskyy, and A. Zolotarova. Precise ^{113}Cd β decay spectral shape measurement and interpretation in terms of possible g_A quenching. *European Physical Journal C*, 84:1158, 2024.
- [6] Heinrich Behrens and Wolfgang Bühring. *Electron radial wave functions and nuclear beta-decay*. Oxford University Press, 1982.
- [7] K. Blaum, S. Eliseev, F. A. Danevich, V. I. Tretyak, Sergey Kovalenko, M. I. Krivoruchenko, Yu. N. Novikov, and J. Suhonen. Neutrinoless double-electron capture. *Rev. Mod. Phys.*, 92:045007, 2020.
- [8] Lucas Bodenstein-Dresler, Yingjie Chu, Daniel Gehre, Claus Gößling, Arne Heimbold, Christian Herrmann, Rastislav Hodak, Joel Kostensalo, Kevin Kröninger, Julia Küttler, Christian Nitsch, Thomas Quante, Ekaterina Rukhadze, Ivan Stekl, Jouni Suhonen, Jan Tebrügge, Robert Temminghoff, Juliane Volkmer, Stefan Zatschler, and Kai Zuber. Quenching of g_A deduced from the β -spectrum shape of ^{113}Cd measured with the COBRA experiment. *Physics Letters B*, 800:135092, 2020. ISSN 0370-2693. doi: <https://doi.org/10.1016/j.physletb.2019.135092>.
- [9] B.A. Brown and W.D.M. Rae. The Shell-Model Code NuShellX@MSU. *Nuclear Data Sheets*, 120:115–118, 2014.
- [10] A. de Roubin, J. Kostensalo, T. Eronen, L. Canete, R. P. de Groote, A. Jokinen, A. Kankainen, D. A. Nesterenko, I. D. Moore, S. Rinta-Antila, J. Suhonen, and M. Vilén. High-precision Q -value measurement confirms the potential of ^{135}Cs for absolute antineutrino mass scale determination. *Phys. Rev. Lett.*, 124:222503, 2020.
- [11] H. Ejiri, J. Suhonen, and K. Zuber. Neutrino–nuclear responses for astro-neutrinos, single beta decays and double beta decays. *Physics Reports*, 797:1, 2019.
- [12] Jonathan Engel and Javier Menéndez. Status and future of nuclear matrix elements for neutrinoless double-beta decay: a review. *Reports on Progress in Physics*, 80(4):046301, 2017. doi: 10.1088/1361-6633/aa5bc5.

- [13] L. Gastaldo, K. Blaum, K. Chrysalidis, and *et al.* The electron capture in ^{163}Ho experiment – ECHO. *Eur. Phys. J. Spec. Top.*, 226:1623–1694, 2017.
- [14] Z. Ge, T. Eronen, K. S. Tyrin, J. Kotila, J. Kostensalo, D. A. Nesterenko, O. Beliuskina, R. de Groote, A. de Roubin, S. Geldhof, W. Gins, M. Hukkanen, A. Jokinen, A. Kankainen, Á. Koszorus, M. I. Krivoruchenko, S. Kujanpää, I. D. Moore, A. Raggio, S. Rinta-Antila, J. Suhonen, V. Virtanen, A. P. Weaver, and A. Zadornaya. ^{159}Dy electron-capture: A new candidate for neutrino mass determination. *Phys. Rev. Lett.*, 127:272301, 2021.
- [15] Z. Ge, T. Eronen, A. de Roubin, K.S. Tyrin, L. Canete, S. Geldhof, A. Jokinen, A. Kankainen, J. Kostensalo, J. Kotila, M.I. Krivoruchenko, I.D. Moore, D.A. Nesterenko, J. Suhonen, and M. Vilén. High-precision electron-capture Q value measurement of ^{111}In for electron-neutrino mass determination. *Physics Letters B*, 832:137226, 2022. ISSN 0370-2693. doi: <https://doi.org/10.1016/j.physletb.2022.137226>.
- [16] P. Gysbers, G. Hagen, J. D. Holt, G. R. Jansen, T. D. Morris, P. Navratil, T. Papenbrock, S. Quaglioni, A. Schwenk, S. R. Stroberg, and K. A. Wendt. Discrepancy between experimental and theoretical β -decay rates resolved from first principles. *Nat. Phys.*, 15:428, 2019.
- [17] M. Haaranen, P. C. Srivastava, and J. Suhonen. Forbidden nonunique β decays and effective values of weak coupling constants. *Phys. Rev. C*, 93:034308, 2016.
- [18] M. Haaranen, J. Kotila, and J. Suhonen. Spectrum-shape method and the next-to-leading-order terms of the β -decay shape factor. *Phys. Rev. C*, 95:024327, 2017.
- [19] L. Hariasz, M. Stukel, P. C. F. Di Stefano, B. C. Rasco, K. P. Rykaczewski, N. T. Brewer, D. W. Stracener, Y. Liu, Z. Gai, C. Rouleau, J. Carter, J. Kostensalo, J. Suhonen, H. Davis, E. D. Lukosi, K. C. Goetz, R. K. Grzywacz, M. Mancuso, F. Petricca, A. Fijałkowska, M. Wolińska-Cichocka, J. Ninkovic, P. Lechner, R. B. Ickert, L. E. Morgan, P. R. Renne, and I. Yavin. Evidence for ground-state electron capture of ^{40}K . *Phys. Rev. C*, 108:014327, Jul 2023. doi: 10.1103/PhysRevC.108.014327.
- [20] L. Hayen, J. Kostensalo, N. Severijns, and J. Suhonen. First-forbidden transitions in reactor antineutrino anomaly. *Phys. Rev. C*, 100:054323, 2019.
- [21] L. Hayen, J. Kostensalo, N. Severijns, and J. Suhonen. First-forbidden transitions in reactor antineutrino spectra. *Phys. Rev. C*, 99:031301, 2019.
- [22] D. K. Keblbeck, R. Bhandari, N. D. Gamage, M. Horana Gamage, K. G. Leach, X. Mougeot, and M. Redshaw. Updated evaluation of potential ultralow Q -value β -decay candidates. *Phys. Rev. C*, 107:015504, 2023.
- [23] O. S. Kirsebom, M. Hukkanen, A. Kankainen, W. H. Trzaska, D. F. Strömberg, G. Martínez-Pinedo, K. Andersen, E. Bodewits, B. A. Brown, L. Canete, J. Cederkäll, T. Enqvist, T. Eronen, H. O. U. Fynbo, S. Geldhof, R. de Groote, D. G. Jenkins, A. Jokinen, P. Joshi, A. Khanam, J. Kostensalo, P. Kuusiniemi, K. Langanke, I. Moore, M. Munch, D. A. Nesterenko, J. D. Ovejas, H. Penttilä, I. Pohjalainen, M. Reponen, S. Rinta-Antila, K. Riisager, A. de Roubin, P. Schotanus, P. C. Srivastava, J. Suhonen, J. A. Swartz, O. Tengblad, M. Vilen, S. Vínals, and J. Äystö. Measurement of the $2^+ \rightarrow 0^+$ ground-state transition in the β decay of ^{20}F . *Phys. Rev. C*, 100:065805, Dec 2019. doi: 10.1103/PhysRevC.100.065805.
- [24] Joel Kostensalo, Jouni Suhonen, Juliane Volkmer, Stefan Zatschler, and Kai Zuber. Confirmation of g_A quenching using the revised spectrum-shape method for the analysis of the ^{113}Cd β -decay as measured with the COBRA demonstrator. *Physics Letters B*, 822:136652, 2021. ISSN 0370-2693. doi: <https://doi.org/10.1016/j.physletb.2021.136652>.
- [25] Joel Kostensalo, Eligio Lisi, Antonio Marrone, and Jouni Suhonen. ^{113}Cd β -decay spectrum and g_A quenching using spectral moments. *Phys. Rev. C*, 107:055502, May 2023. doi: 10.1103/PhysRevC.107.055502.
- [26] Joel Kostensalo, Eligio Lisi, Antonio Marrone, and Jouni Suhonen. Analysis of ^{115}In β decay through the spectral moment method. *Physical Review C*, 110:045503, 2024.
- [27] Anil Kumar, Praveen C. Srivastava, Joel Kostensalo, and Jouni Suhonen. Second-forbidden nonunique β^- decays of ^{24}Na and ^{36}Cl assessed by the nuclear shell model. *Phys. Rev. C*, 101:064304, Jun 2020. doi: 10.1103/PhysRevC.101.064304.
- [28] Anil Kumar, Praveen C. Srivastava, and Jouni Suhonen. Second-forbidden nonunique β^- decays of $^{59,60}\text{Fe}$: possible candidates for g_A sensitive electron spectral-shape measurements. *The European Physical Journal A*, 57:225, 2021. ISSN 1434-601X. doi: 10.1140/epja/s10050-021-00540-6.
- [29] K. Langanke and G. Martínez-Pinedo. Nuclear weak-interaction processes in stars. *Rev. Mod. Phys.*, 75:819–862, Jun 2003. doi: 10.1103/RevModPhys.75.819.
- [30] K Langanke, G Martínez-Pinedo, and R G T Zegers. Electron capture in stars. *Reports on Progress in Physics*, 84(6):066301, may 2021.
- [31] A. F. Leder, D. Mayer, J. L. Ouellet, F. A. Danevich, L. Dumoulin, A. Giuliani, J. Kostensalo, J. Kotila, P. de Marcillac, C. Nones, V. Novati, E. Olivieri, D. Poda, J. Suhonen, V. I. Tretyak, L. Winslow, and A. Zolotarova. Determining g_A/g_V with high-resolution spectral measurements using a LiInSe_2 bolometer. *Phys. Rev. Lett.*, 129:232502, Dec 2022. doi: 10.1103/PhysRevLett.129.232502.
- [32] L. Pagnanini, G. Benato, P. Carniti, E. Celi, D. Chiesa, J. Corbett, I. Dafinei, S. Di Domizio, P. Di Stefano, S. Ghislandi, C. Gotti, D. L. Hellis, R. Knobel, J. Kostensalo, J. Kotila, S. Nagorny, G. Pessina, S. Pirro, S. Pozzi, A. Puiu, S. Quitadamo, M. Sisti, J. Suhonen, and S. Kuznetsov. Simultaneous measurement of the half-life and spectral shape of ^{115}In β decay with an indium iodide cryogenic calorimeter. *Phys. Rev. Lett.*, 133:122501, Sep 2024. doi: 10.1103/PhysRevLett.133.122501.
- [33] M. Paulsen, P. C.-O. Ranitzsch, M. Loidl, M. Rodrigues, K. Kossert, X. Mougeot, A. Singh, S. Leblond, J. Beyer, L. Bockhorn, C. Enss, M. Wegner, S. Kempf, and O. Nähle. High precision measurement of the ^{99}Tc β spectrum. *Physical Review C*, 110:055503, 2024.
- [34] M. Ramalho and J. Suhonen. Computed total β -electron spectra for decays of Pb and Bi in the $^{220,222}\text{Rn}$ radioactive chains. *Phys. Rev. C*, 109:014326, Jan 2024. doi: 10.1103/PhysRevC.109.014326.
- [35] M. Ramalho, Z. Ge, T. Eronen, D. A. Nesterenko, J. Jaatinen, A. Jokinen, A. Kankainen, J. Kostensalo, J. Kotila, M. I. Krivoruchenko, J. Suhonen, K. S. Tyrin, and V. Virtanen. Observation of an ultralow- Q -value electron-capture channel decaying to ^{75}As via a high-precision mass measurement. *Phys. Rev. C*, 106:015501, 2022.
- [36] M. Ramalho, J. Suhonen, J. Kostensalo, G. A. Alcalá, A. Algora, M. Falot, A. Porta, and A.-A. Zakari-Issoufou. Analysis of the total β -electron spectrum of ^{92}Rb : Implications for the reactor flux anomalies. *Phys. Rev. C*, 106:024315, 2022.
- [37] M. Ramalho, J. Suhonen, A. Neacsu, and S. Stoica. Spectral shapes of second-forbidden single-transition nonunique β decays assessed using the nuclear shell model. *Frontiers of Physics*, 12:1455778, 2024.
- [38] Marlon Ramalho and Jouni Suhonen. g_A -sensitive β spectral shapes in the mass $A = 86 - 99$ region assessed by the nuclear shell model. *Phys. Rev. C*, 109:034321, Mar 2024. doi: 10.1103/PhysRevC.109.034321.
- [39] M. Redshaw. Precise Q value determinations for forbidden and low energy β -decays using penning trap mass spectrometry. *Eur. Phys. J. A*, 59:18, 2023.
- [40] J. Ruotsalainen, M. Stryczyk, M. Ramalho, T. Eronen, Z. Ge, A. Kankainen, M. Mougeot, and J. Suhonen. Ultra-low q_β value for the allowed decay of $^{110}\text{ag}^m$ confirmed via mass measurements, 9 2024.
- [41] Stefan Schoppmann. Status of anomalies and sterile neutrino searches at nuclear reactors. *Universe*, 7(10):360, 2021. ISSN 2218-1997. doi: 10.3390/universe7100360. URL <https://www.mdpi.com/2218-1997/7/10/360>.
- [42] Jouni Suhonen. *From Nucleons to Nucleus: Concepts of Microscopic Nuclear Theory*. Springer Berlin, Heidelberg, 2007.
- [43] Jouni Suhonen. Impact of the quenching of g_A on the sensitivity of $0\nu\beta\beta$ experiments. *Phys. Rev. C*, 96:055501, 2017.
- [44] Jouni Suhonen and Joel Kostensalo. Double β decay and the axial strength. *Frontiers in Physics*, 7:29, 2019. ISSN 2296-424X.
- [45] Jouni T. Suhonen. Value of the Axial-Vector Coupling Strength in β and $\beta\beta$ Decays: A Review. *Frontiers in Physics*, 5:55, 2017.
- [46] Surender, Vikas Kumar, and Praveen C. Srivastava. Study of β^+/EC -decay properties of sd shell nuclei using nuclear shell model. *Annals of Physics*, 470:169772, 2024. ISSN 0003-4916. doi: <https://doi.org/10.1016/j.aop.2024.169772>.
- [47] E. Ydrefors, M.T. Mustonen, and J. Suhonen. MQPM description of the structure and beta decays of the odd $A=95,97$ Mo and Tc isotopes. *Nuclear Physics A*, 842(1):33–47, 2010. ISSN 0375-9474. doi: <https://doi.org/10.1016/j.nuclphysa.2010.04.005>.
- [48] Chao Zhang, Xin Qian, and Muriel Falot. Reactor antineutrino flux and anomaly. *Progress in Particle and Nuclear Physics*, 136:104106, 2024.